

Beyond the Nanomaterials Approach: Influence of Culture Conditions on the Stability and Antimicrobial Activity of Silver Nanoparticles

Roberto Vazquez-Muñoz, Nina Bogdanchikova, and Alejandro Huerta-Saquero*



Cite This: *ACS Omega* 2020, 5, 28441–28451



Read Online

ACCESS |



Metrics & More

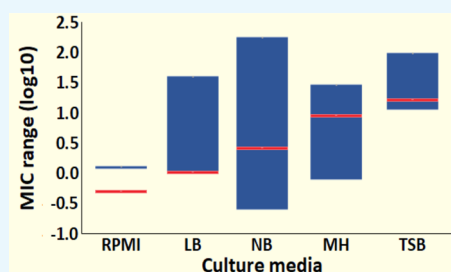


Article Recommendations



Supporting Information

ABSTRACT: Silver nanoparticles (AgNPs) as antimicrobial agents have been extensively studied. It is generally assumed that their inhibitory activity heavily depends on their physicochemical features. Yet, other parameters may affect the AgNP traits and activity, such as culture medium composition, pH, and temperature, among others. In this work, we evaluated the effect of the culture medium physicochemical traits on both the stability and antibacterial activity of AgNPs. We found that culture media impact the physicochemical traits of AgNPs, such as hydrodynamic size, surface charge, aggregation, and the availability of ionic silver release rate. As a consequence, culture media play a major role in AgNP stability and antimicrobial potency. The AgNP minimal inhibitory concentration (MIC) values changed up to 2 orders of magnitude by the influence of culture media alone when single-stock AgNPs were tested on the same strain of *Escherichia coli*. Furthermore, a meta-analysis of the AgNP MIC values confirms that the “chemical complexity” of culture media influences the AgNP activity. Studies that address only the antimicrobial activities of nanoparticles on common bacterial models should be performed by standardized susceptibility assays, thus generating replicable, comparable reports regarding the antimicrobial potency of nanomaterials.



1. INTRODUCTION

Silver nanoparticles (AgNPs) are among the most studied and produced nanomaterials worldwide due to their wide range of applications. AgNPs are key components in hundreds of commercial products, such as paints, coatings, electronics, cosmetics, health care (nanopharmaceuticals), and more.^{1–3} In medicine, AgNPs are of particular interest due to their potent antimicrobial activity against viruses,^{4,5} bacteria,^{6,7} and fungi,^{8,9} among others. Moreover, AgNPs may exhibit synergistic effects with antibiotics and can be applied as sanitizers, which increase their relevance.^{10–12}

Therefore, understanding and properly establishing their antimicrobial potency and toxicity are of utmost relevance. As with common antibiotics, the antimicrobial activity of AgNPs is usually determined by assessing the minimal inhibitory concentration (MIC) or the minimal effective concentration (MEC), which can be an experimental or calculated endpoint value. The MIC can be assessed through diverse methods, which may consider different criteria, with the CLSI and EUCAST guidelines being the most common. Regarding their toxicity, there are several guidelines to address it¹³ as well as different works aiming to assess their toxicity.^{14,15} However, it is not uncommon to find a plethora of different methods for evaluating and interpreting the antimicrobial activity and the toxicity of AgNPs. Although it is true that some strains or particular experimental setups may need specific culture conditions, it is not uncommon to find articles that use a

wide array of different conditions for assessing the AgNP antimicrobial activity on common bacterial models, such as *Escherichia coli*.

Understanding the AgNPs' antimicrobial activity and their potential toxicity is critical for improving their current and future applications as well as for dealing with any potential risk to health and the environment. Yet, the different culture conditions used for assessing the antimicrobial activity of AgNPs lead to challenges regarding the understanding of their potency, mechanisms of action, stability, etc. Moreover, the lack of consistency in the susceptibility assays may even lead to reproducibility issues as some of the published results may not be readily replicated under a different experimental setup. In the literature, among the variations in culture conditions are initial inoculum size,^{16,17} incubation time,¹⁸ and the culture media.^{19–21}

Culture media are a key factor as their formulation may include different concentrations of proteins, sugars, and inorganic salts, among others. Moreover, their different physicochemical characteristics provide them with different

Received: April 30, 2020
Accepted: August 17, 2020
Published: October 26, 2020



pH values, ionic strength, redox potential, etc. Consequently, due to their very different chemical composition, culture media are complex systems that influence the biological behavior of cells and may alter the potency of antimicrobials.

Regarding AgNPs and other silver species, some of their interactions with culture media and their components have been reported by several authors. When culture media interact with AgNPs, they may affect their properties in different ways, such as the silver ion release rate, aggregation, or surface oxidation process.^{22,23} Biomolecules, salts, and other culture medium components destabilize the nanoparticles,^{24,25} whereas proteins produce protein corona,^{26,27} which may affect their antimicrobial activity.^{28–32} Also, parameters such as salinity and pH impact AgNPs,^{33,34} particularly their stability in aqueous solutions.^{35–37}

However, up to now, these studies have not shown a potential correlation between the physicochemical properties, stability, and the antimicrobial activity of AgNPs under different culture conditions. Back in 2011, MacCuspie concluded that no clear trends are found between the AgNP properties, stability, and activity,³⁸ and recently, although it has been suggested several times that the culture medium may affect the AgNP antimicrobial potency,^{31,39} still, no clear trends have been found. Furthermore, it is still assumed that the antimicrobial activity of the AgNPs relies almost exclusively on nanoparticle physicochemical traits rather than on the cell–nanoparticle–environment interactions. This idea has led to an incomplete comprehension of the AgNP activity and weakens the capacity to compare its antimicrobial activity and potential toxicity.

In this work, we hypothesized that the influence of culture media on the stability and antimicrobial activity of AgNPs is related to the “chemical complexity” of culture media. The aim was to establish a possible correlation between the chemical composition of the culture medium, as a complex system, the AgNPs’ physicochemical traits, and their antimicrobial activity. Although the culture medium components and nanomaterial interactions have been addressed, the consequences of these interactions on the biological activity of AgNPs have not been correlated under the cell–nanoparticle–environment complex system approach. To achieve our goal, we evaluated the effect of five different culture media (NB, LB, MH, TSB, and RPMI) on the antimicrobial activity of AgNPs, using the same microbial strain (*E. coli*) and the same AgNPs. Additionally, a comparative meta-analysis of the literature was performed to contrast our experimental data with the available information. The role of culture media regarding toxicity assays of AgNPs is discussed.

2. RESULTS AND DISCUSSION

2.1. Culture Media and Their Components Change the Stability of AgNPs. 2.1.1. AgNP Surface Plasmon Changes under Different Culture Media.

AgNPs, in Milli-Q water, display the expected UV–vis absorbance profile with a single peak, typical for silver nanoparticles, with a maximum at $\lambda = 415$ nm (Figure 1); also, the UV–vis profile of AgNO₃ was measured, displaying a profile with a maximum at $\lambda = 290$ nm.

The absorbance of AgNPs in different culture media showed variations in intensity, position, and shape. At $t = 0$, AgNPs diluted with different culture media displayed minor differences in their surface plasmon (Figure 2A). However, the surface plasmon displayed a noticeable decrease from the AgNPs suspended in YPD. AgNPs in LB, YPD, and TSB show

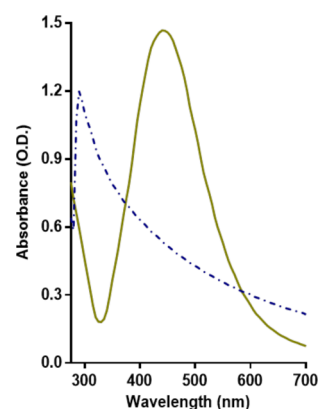


Figure 1. Culture medium components change the UV–vis spectra of the AgNPs. UV–vis spectra of AgNPs and AgNO₃ in deionized water.

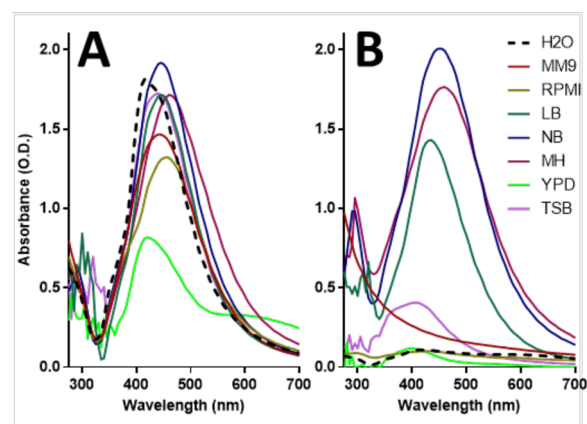


Figure 2. Culture medium components change the UV–vis spectra of the AgNPs. UV–vis spectra of AgNPs when exposed to different culture media, at $t = 0$ h (A), and after 24 h of incubation, $t = 24$ h (B).

small, low-intensity peaks around the λ_{300} band, which has been associated with the presence of other silver species and nanoclusters.⁴⁰ AgNPs in RPMI and NB show a small shoulder toward the blueshift, while those in YPD display a broad shoulder toward the redshift, which may suggest that nanoparticles are disintegrating and agglomerating, respectively. Baset et al. showed how the shift of the peak reveals if AgNPs are clustering or becoming smaller.⁴¹

At $t = 24$ h, the variations in the surface plasmon were more evident, which suggests that the physicochemical properties and stability of AgNPs were affected (Figure 2B). The AgNP absorbance intensity reduction (in MM9, RPMI, TSB, and YPD) and the redshift in the absorbance (in NB) suggest that nanoparticles may be precipitating or aggregating over time. Also, the full width at half-maximum (FWHM) of the absorbance peak of AgNPs is broadening at $t = 24$ h (in NB and MH), which suggests that AgNPs are more polydisperse, possibly due to oxidizing processes.⁴² However, the FWHM of AgNPs decreased in LB, suggesting that the reduction of the nanoparticles was predominant and that nanoparticles are transitioning to be monodisperse. Moreover, there was a blueshift in the surface plasmons of AgNPs in MM9, YPD, and TSB, suggesting that nanoparticles may be disintegrating, favoring the release of silver species. AgNPs in NB and MH show an increment in the intensity in the λ range between 300 and 400 nm, which may suggest an increase in the relative

concentration of other silver species. In Figure S1, the individual graphs for the AgNPs suspended in each culture medium, at $t = 0$ h and 24 h, are provided.

The distinctive chemical composition and pH found in the different culture media lead to unique interactions with the AgNPs, changing their physicochemical properties, as revealed by the surface plasmon. These changes may be predominantly caused by fast and spontaneous physicochemical interactions – redox processes, passivation, or chemical bonding, among others – with the culture medium components. The predominant components for most culture media are proteins/amino acids, reducing sugars, and salts, which are known to interact with metals.

2.1.2. Protein Concentration Influences AgNP Stability.

For AgNPs suspended at low peptone concentrations, the surface plasmons were similar to the profile of the control (AgNPs in Milli-Q water). In contrast, AgNPs in the solution with the highest concentration of peptone (5.24%) showed different surface plasmon (Figure 3A). The intensity of the

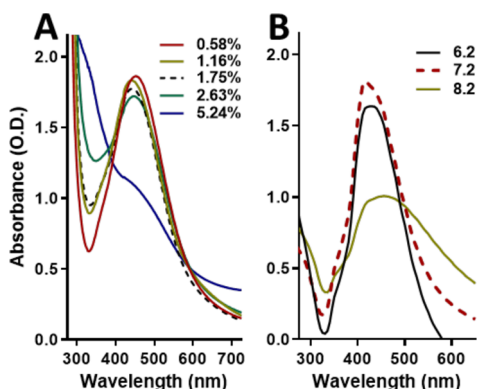


Figure 3. Different pH values change the UV–vis spectra of the AgNPs. Absorption spectra of the AgNPs exposed to deionized water with different concentrations of peptone (A) and exposed to different pH (B).

peak decreased and shifted toward blue, although a small shoulder at λ_{415} is kept. The change in the profile may be due to the precipitation of AgNPs. Also, AgNPs may dissolve, leading to the formation of other silver species, as suggested by the broadening of the peak below 400 nm. This corresponds to observations in the literature, which indicate that cysteine can passivate AgNPs due to the formation of chemical bonds with the silver ions.^{43–45} Also, proteins may adsorb Ag(I) and dissolve the AgNPs.^{32,46} Additionally, it has been widely reported that the AgNP–protein interaction leads to the “protein corona” formation around the AgNPs.⁴⁷ Protein corona induces changes in the AgNPs’ traits, such as size, stability, and even in the way they interact with cells.²⁶ Hence, proteins and some amino acids alter the physicochemical properties of the AgNPs, which may impact their stability. This observation may be of special interest when producing AgNPs via green synthesis as the proteinic content from the extracts directly impacts the AgNPs; therefore, if the protein content is not consistent, the properties of the nanoparticles may be compromised.⁴⁸

2.1.3. The Stability of AgNPs Depends on the Acidic/Alkaline Environment. The surface plasmon of AgNPs in an acidic pH (6.2) solution was similar to the profile of AgNPs in the control solution (pH 7.2) (Figure 3B), although it showed

a reduction in intensity and a slight shift to red. In contrast, AgNPs in the basic pH (8.2) solution showed a different surface plasmon. The peak wideness increased and exhibited a slightly shift to red, suggesting an increasing oxidation and size polydispersity. Also, the noticeable reduction in intensity and the emergence of a small shoulder around λ_{350} suggest that AgNPs may be dissolving. Therefore, the silver ion release rate may be favored in alkaline environments, leading to faster degradation of the AgNPs, but the release decreases in acidic environments.³⁶ Nevertheless, some authors suggest the opposite effect: acidic environments reduce the stability of silver nanoparticles, whereas the stability is maintained in an alkaline environment. Goswami et al. reported that AgNP stability was higher in a basic solution (pH 9) than in the acidic one (pH 5).³⁵ Similarly, Qu et al. found that AgNPs became unstable in pH 2 but remained unaffected at pH 12.³⁷ Then, solutions with extreme pH values may have different effects on AgNP stability as the ion release, oxidation state, and other chemical effects may interact simultaneously. Additionally, the pH can alter the ionic strength in a solution, and an increase in the ionic strength leads to the destabilization of the AgNPs.²⁵ Also, an increase in ionic strength promotes the aggregation of chemically synthesized AgNPs, whereas the opposite effect has been observed in biologically synthesized AgNPs.⁴⁹ Therefore, the impact of pH on nanoparticles may be attributed to their characteristics, such as coating agent, size, and shape, among others.

For this study, the pH values were chosen according to the recipes for culture medium preparation. Culture medium pH values usually range between 6.5 and 7.5, being around 7.2 for most bacterial models, such as *E. coli*. Based on our results, it seems that pH plays only a minor role in the AgNP stability when the experiments are performed under environments close to pH 7. A further study, on a more complete scale of pH, may provide a deeper insight into the influence of pH on the behavior of AgNPs beyond the scope of the culture medium conditions.

2.1.4. The Culture Media Change the Hydrodynamic Size and ζ -Potential of AgNPs.

DLS spectroscopy analysis shows that AgNPs diluted in Milli-Q water have a polydispersity index (PDI) of 0.247. The PDI implies that AgNPs have a moderate polydispersity, yet most of them are within a major, single population size. The AgNPs’ ζ -potential is -14.1 mV; therefore, their surface is negatively charged due to the PVP coating. A ζ -potential value of ≥ 30 mV is generally accepted as the limit of stability.⁵⁰ According to our results, the ζ -potential value suggests that the AgNP suspension has relatively moderate stability. AgNPs have a hydrodynamic size of 95.3 nm. A previous characterization from our group¹⁵ showed that these AgNPs have an average size of 35 ± 15 nm. Thus, their hydrodynamic size is more than 2 times greater than their metallic core. The large hydrodynamic size of the AgNPs may be partly due to the PVP coating, which expands when AgNPs are in an aqueous solution. Moreover, the previous TEM analysis does not provide any evidence of AgNP initial aggregation ($t = 0$ h), although the low ζ -potential value may be an indication that they slowly aggregate over time. At $t = 24$, the DLS analysis revealed the presence of AgNPs in suspension despite that UV–vis spectrophotometry showed that their surface plasmon intensity was noticeably reduced. The original stocks of these PVP–AgNPs are stable for months, according to our observations. No precipitate formation was perceived in the container, and both the surface

plasmon and antimicrobial activity remain practically unchanged over time (at least for 20 months). This stability may be influenced by the PVP, which acts as a dispersant, prevents aggregation, and acts as a reducing agent, preventing the reduction of the PVP.⁵¹

All nanoparticles used in this study came from the same stock, yet when suspended in different culture media, they exhibited variations in their hydrodynamic diameter (Figure 4A) and ζ -potential (Figure 4B). Regarding the hydrodynamic

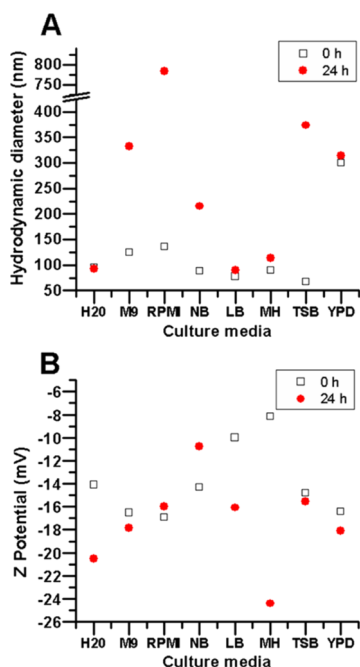


Figure 4. Culture media affect the size and charge of the AgNPs. Hydrodynamic size (A) and ζ -potential (B) of AgNPs when diluted in different culture media.

size, at $t = 0$ h, changes in the AgNP size were more noticeable for some culture media than in others. AgNPs in NB and MH displayed a hydrodynamic size similar to the control (Table S1). In LB and TSB, AgNPs displayed a hydrodynamic size smaller than AgNPs in Milli-Q water (87.8 and 67.4 nm, respectively). Both culture media have different chemical compositions; however, they share a high concentration of added inorganic salts (0.5 and 0.75%, respectively), but the protein content is higher in TSB, as described in Table S2. In these media, the salts may be hindering the interactions with proteins and other components avoiding protein corona formation.

In contrast, AgNPs in M9, RPMI, and YPD displayed a hydrodynamic size larger than in the control (124.5, 136.2, and 299.6 nm, respectively). In particular, AgNPs in YPD displayed a hydrodynamic size 3 times larger than the control. YPD has a high content of proteins, no added salts, and a high content of reducing sugars (2%), which may favor protein corona formation and also lead to rapid aggregation and precipitation of AgNPs. This matches the observation from their surface plasmon (Figure 2A), in which a broad shoulder emerges between 500 and 700 nm, evidence of larger nanoparticles. This phenomenon resembles an observation from Kvitek et al., where the profile intensity and shape were affected by the ascending concentration of poly(diallyl-dimethyl-ammonium) chloride, a cationic polyelectrolyte.⁵³ They showed that the

maximum peak of AgNP absorbance decreased as the hydrodynamic size increased, while other peaks were rising at $\lambda > 500$ nm, confirming the increase of AgNP size and polydispersity. However, M9 and RPMI have a very low content of proteins/amino acids and sugars and a high content of salts (around 1%). It is unclear why the hydrodynamic size of AgNPs increased (around 30% larger). This observation does not correlate with their surface plasmon as they are similar to the profile control (in Milli-Q water), although some differences were observed. At $t = 24$ h, the AgNP hydrodynamic size in Milli-Q water, as well as AgNPs in LB and MH, was similar to the size at $t = 0$. For AgNPs in LB and MH, the surface plasmon at $t = 24$ h was also comparable to their corresponding profiles at $t = 0$ h. An increase in the AgNP hydrodynamic size was observed in M9, RPMI, NB, TSB, and YPD. For AgNPs in M9, RPMI, YPD, and TSB (332.4, 784.2, 314, and 373.5 nm, respectively), these changes match the intensity decrease of their surface plasmon (Figure 2B). Interestingly, AgNPs in NB showed a slight increase in the hydrodynamic size (215 nm), whereas their UV–vis absorbance profile remained almost unchanged.

At $t = 0$ h, the polydispersity index (PDI) of AgNPs is between the 0.2 and 0.3 range in water and most culture media, but in RPMI, the PDI of AgNPs is higher (0.621) (Table S1). However, at $t = 24$ h, the PDI values increased in most culture media (between the 0.3 and 0.4 range), except in RPMI and NB, which showed a decrease regarding their corresponding values at $t = 0$ h. As the PDI represents the distribution of size populations within the sample, the obtained values revealed that the size distribution was moderately uniform in most samples at $t = 0$ h and remained relatively close to the monodispersity threshold at $t = 24$ h in NB, TSB, and RPMI, whereas those in LB, MH, and YPD increased, which provides additional evidence that hydrodynamic size of the AgNPs changes under different conditions (Figure S4). The closer the PDI values are to zero, the more uniform is the size of the particles within the samples. Usually, PDI values below 0.2 are considered to represent a monodispersity distribution.⁵² Our values were close to the limit of 0.2 at $t = 0$ h, and although their polydispersity changed at $t = 24$ h, they remained relatively within a major population size.

Regarding ζ -potential, there were noticeable variations in the different culture media over time (Figure 4B). However, nanoparticles maintained a negative surface charge under all conditions (Table S1). At $t = 0$ h, the ζ -potential absolute value remained similar to that of the control (114.1 mV) for AgNPs in NB, and TSB, showing a decrease in the ζ -potential absolute value in LB and MH. Interestingly, the surface plasmons in these culture media were similar to those in the control at $t = 0$ h. AgNPs in M9, RPMI, and YPD showed a slight increase in the ζ -potential absolute value. The AgNPs in these culture media also exhibited an evident reduction in their surface plasmon intensity at $t = 0$ h. Particularly, AgNPs in YPD also displayed a noticeable decrease and the emergence of a shoulder starting at λ_{500} nm. At $t = 24$ h, the ζ -potential absolute value of AgNPs in Milli-Q water increased to 120.5 mV, which is contrary to the expected based on the intensity reduction of their surface plasmon. However, as described above, their hydrodynamic size remained practically unchanged at $t = 0$ h. The potential causes of the differences observed between the UV–vis spectrophotometry analysis and the DLS results remain to be further explored. For AgNPs in the culture media, all the ζ -potential absolute values were

different at $t = 24$ h (Table S1). For AgNPs in M9, RPMI, and TSB, the ζ -potential absolute values remained close to their values at $t = 0$ h, which contradicts the observations from both their surface plasmon and hydrodynamic size, which were noticeably different over time. For YPD, AgNPs' ζ -potential absolute value was also similar to the $t = 0$ h, which is also true for their HS; however, their surface plasmons were noticeably different over time. AgNPs in NB showed a decrease in the ζ -potential absolute value regarding the initial time, suggesting loss of stability. This matches the aggregation observed for their hydrodynamic size over time, although the surface plasmon remained stable at $t = 24$ h. AgNPs in LB and MH displayed higher ζ -potential absolute values, which suggest an increase in stability, particularly in MH. This is similar to the observations from their surface plasmon and hydrodynamic size, which remained very similar regarding the $t = 0$ h.

Some of the culture media with similar chemical components, such as LB and YPD, exert a very different impact on the AgNP ζ -potential, hydrodynamic size, and surface plasmon. In contrast, culture media with different compositions, such as MH and LB, have a similar, marginal effect on the AgNP surface plasmon, ζ -potential, and hydrodynamic size. The optical characterizations (UV-vis spectrophotometry and DLS) remain consistent for determining the AgNP stability (LB and MH) or instability (M9, RPMI, and TSB) over time. In contrast, for AgNPs in NB and YPD, there is not an evident trend as the data from the optical characterization are not consistent and cannot be correlated with our current data. AgNPs are subject to instant physicochemical interactions with the culture medium components that alter their surface chemistry. These interactions lead to changes in hydrodynamic size, stability, and surface plasmon, suggesting aggregation, disintegration, and different redox processes over time.

Also, a future study considering the protein corona formation on different media may expand the explanation and shed some light on the matter. LB, NB, MH, YPD, and TSB contain proteins from different sources. For MH, YPD, and TSB, the protein content is particularly high (2 to 3%); therefore, they are more likely to form protein corona on the AgNPs. However, the stability of AgNPs was only negatively impacted on TSB and YPD. Yet, intriguingly, they exhibited a different behavior regarding their hydrodynamic size: MH remained unchanged over time, with a hydrodynamic size similar to the control, AgNPs in TSB exhibited a reduction in their hydrodynamic size at $t = 0$ h (67 nm), but noticeably increased at $t = 24$ h (374 nm), whereas for YPD, there was an increase in their HS at $t = 0$ h (300 nm) keeping hydrodynamic size at $t = 24$ h (314 nm). TSB and YPD also have a high content of other components, 2% of sugars for YPD, and 0.75% of salts for TSB, which may also play a role in the AgNP chemistry and even in the protein corona formation.

Therefore, different and diverse mechanisms and interactions may be simultaneously present due to the diversity of the culture medium components. Moreover, these interactions may be influenced by the traits of the AgNPs (size, shape, surface charge) and even the presence and nature of a coating agent, which alter the surface chemistry of the AgNPs. In this study, AgNPs are coated with PVP, which acts as a dispersant, confers stability, and also acts as a reducing agent, and it may confer resilience against some of the chemical effects from the culture medium components.²⁴ However, as the culture medium is more than the sum of its components and pH, it

is difficult to predict how it will impact the stability and optical properties of the AgNPs.

2.1.5. The Silver Content and the Silver Ion Release Rate Depend on the Culture Media. ICP-OES analysis was performed to evaluate the silver content of centrifuged media (Figure 5). At $t = 0$ h, the lowest silver content was in RPMI

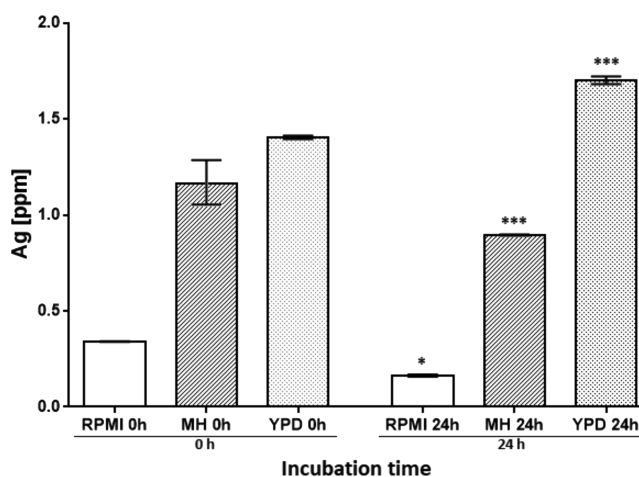


Figure 5. Silver content variations in different culture media, at 0 and 24 h of incubation. There are significant differences in the silver content in the different culture media over time. One-way ANOVA was performed on the replicates of each treatment followed by Tukey's multiple comparison post-test, using the software OriginPro 8 (OriginLab), * = $p < 0.05$, *** = $p < 0.001$.

(0.34 ppm), while the highest was in YPD (1.41 ppm). At $t = 24$ h, the silver content was significantly different in the culture media. The silver content decreased in RPMI and MH (0.17 and 0.89 ppm, respectively) but increased in YPD (1.7 ppm) (Table S3). Therefore, the silver ion release rate and behavior are different in each culture media, being more readily released in RPMI and MH than in YPD; thus, the silver content in the pellet (AgNPs) is lower.

To corroborate that AgNPs were precipitated by centrifugation, the supernatant of each culture medium was analyzed by UV-vis spectrophotometry after centrifugation. UV-vis analysis revealed that the typical profile of the AgNPs was not observed in any supernatant, at $t = 0$ h. At $t = 24$ h, the AgNP absorbance profile was not observed in RPMI and MH, but the YPD supernatant revealed the typical profile of the AgNPs but with a very low intensity ($OD_{415nm} < 0.3$). A possible explanation could be that YPD has a high dextrose content, a reducing sugar, which may interact with the silver ions from the supernatant, favoring the AgNP formation, as reported elsewhere.⁵⁴ Additionally, the UV-vis analysis of the supernatant revealed the presence of non-nanostructured silver species, below λ_{300} , according to the literature⁴⁰ (Figure S2). The formation of different silver species may be due to the interaction of the silver ions with the culture medium components, and the silver species continue to bind to them after centrifugation, remaining in the supernatant. For each condition, the corresponding culture medium, centrifuged, with no AgNPs, was used as a blank in the UV-vis spectroscopy analysis; therefore, the absorbance profile obtained is the result of the interaction of silver with the culture media.

2.1.6. The Concept of Chemical Complexity of the Culture Media. At this point, it is evident that culture media influence

the AgNP size, surface charge, ion release, and, therefore, their stability. Culture media are formulated using a wide array of chemical components; therefore, they have a varying degree of chemical complexity. For this study, we set chemical complexity as the relative quantity and chemical diversity of the culture medium components. The pH value was also considered. This “complexity” ranges from the defined – synthetic – media (such as M9 or RPMI) to the nondefined – complex – media (such as LB and MH). The straightforward relationship between the observed changes in AgNPs and the culture medium composition has yet to be addressed due to the multiple interactions among the components, exposition to light, temperature, ionic strength, and interaction with salts, among others.

We observed consistency between the changes in the optical characterization of the AgNPs and their stability for some culture media, yet for others, a not evident trend was observed. However, although it may be difficult to predict the impact of culture media on AgNPs, the effects on their stability and morphology are clear. Then, what are the consequences of these changes on antimicrobial activity? We addressed this issue below.

2.2. Culture Media Determine the Antimicrobial Activity of AgNPs. **2.2.1. Culture Medium Composition Impacts *E. coli* Growth.** Bacterial growth with no AgNPs in the peptone-/dextrose-modified MH was measured. Our results reveal that *E. coli* displayed significantly different growth in the peptone-/dextrose-modified MH (Figure 6).

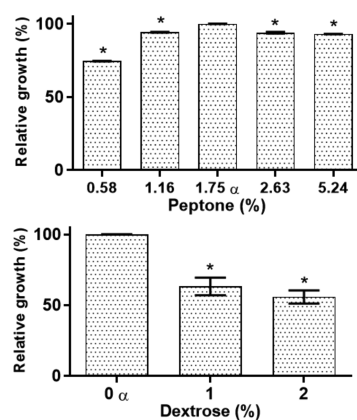


Figure 6. Culture medium components impact the growth of *E. coli*. *E. coli* growth in MH broth under standard conditions, with variations in peptone and dextrose concentrations. There are significant differences in microbial growth. One-way ANOVA with the Holm–Sidak post-test, * = $p < 0.05$. α = MH reference media (containing 1.75% peptone and 0% dextrose).

Moreover, an interesting observation is that *E. coli* showed the best growth under the standard MH formulations, which are 1.75% peptone and no dextrose. This was contrary to the projected as it was expected that *E. coli* would grow better in the enriched MH.

***E. coli* Growth Is Influenced by the Culture Media.** The growth of *E. coli* incubated in different culture media with no AgNPs was determined. Our results show that there are significant differences in microbial fitness even before the use of any antimicrobial treatment. The highest bacterial growth was observed in TSB broth (>200%), while the lowest in RPMI (<50%) (Figure 7). These disparities in bacterial growth under different culture media should be relevant when

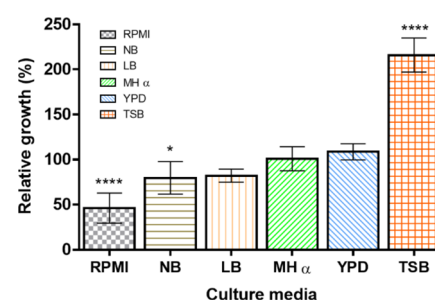


Figure 7. Effect of culture media on bacterial growth. *E. coli* was cultured in different media, with no AgNPs. Growth in MH was set as 100%. One-way ANOVA was performed on the replicates of each treatment followed by Tukey’s multiple comparison post-test, using the software OriginPro 8 (OriginLab), * = $p < 0.05$, **** = $p < 0.001$.

comparing susceptibility assays from different experimental setups. Moreover, our results highlight that any variation in the culture media conditions modifies both the AgNP stability and bacterial growth. Furthermore, these variations suggest that there may be misleading interpretations regarding the antimicrobial activity, particularly if no additional controls are used.

2.2.3. The Antimicrobial Activity of AgNPs Is Influenced by the Components of the Culture Media. The effects of AgNPs on *E. coli* grown in peptone- or dextrose-modified MH were assessed. The lowest AgNP MIC was found in the lowest concentrations of peptone (0.58%) and dextrose (0%), with MICs of <7.5 and 10 $\mu\text{g mL}^{-1}$, respectively (Table 1). On the

Table 1. AgNP MICs on *E. coli* when Cultured on Modified MH

peptone (%)	MIC ($\mu\text{g mL}^{-1}$)	dextrose (%)	MIC ($\mu\text{g mL}^{-1}$)
0.58	<7.5	0 ^a	12.5
1.16	12.5	1	>20
1.75 ^a	12.5	2	>20
2.63	17.5		
5.24	20		

^aMH standard formulation.

other hand, the highest MICs were found for the highest concentrations of peptone (5.24%) and dextrose (2%), with MICs of 20 and >20 $\mu\text{g mL}^{-1}$, respectively. This is an interesting finding because the AgNP MIC values raised proportionally as the concentration of dextrose or peptone increased. Nevertheless, for *E. coli* in modified MH broth with no AgNPs, the growth decreased when the concentration of peptone/dextrose was higher than in the standard formulations (Figure 6). Hence, although the bacteria had a lower fitness at high concentrations of peptone and dextrose, the MIC values increased. Therefore, peptone and dextrose are hindering the AgNP antimicrobial potency. This must be considered when culture media are prepared as sometimes they are enriched without considering the effect of culture media on AgNPs.

2.2.4. The MIC of AgNPs Depends on Culture Media. The AgNPs displayed diverse MIC values in different culture media. The lowest MIC was 0.25 $\mu\text{g mL}^{-1}$ for RPMI, while the highest was 15 $\mu\text{g mL}^{-1}$, for TSB, whereas for MH, the MIC was 12.5 $\mu\text{g mL}^{-1}$. The MIC variations were caused by the culture medium components, which impaired the silver ion release, reducing its bioavailability and dissolving/aggregating

the nanoparticles, among other effects. Therefore, although the same stock of AgNPs and bacterial strain were used and they were tested under identical culture conditions, the MIC varied up to 2 orders of magnitude just by the influence of the culture media (Table S4). It is relevant to remark that our experimental MIC values increased correspondingly as the chemical complexity of the culture media augmented, as follows: RPMI, LB, NB, MH, and TSB. Although this hierarchical organization is arbitrary, as explained earlier (Section 2.1.6), it correlates the AgNP antibacterial activity with the chemical complexity of the culture media. Moreover, it also correlates with bacterial growth in different culture media (Figure 7).

Furthermore, from the literature meta-analysis, we obtained the AgNP MIC values against *E. coli*. These MIC values were grouped by culture media; then, the MIC ranges were determined for each group (Table S2). The culture media were assorted according to our concept of chemical complexity, described before (Section 2.1.6). The average values from the literature also increased as the culture media become more “chemically complex”. Therefore, our experimental results and the meta-analysis corroborate the influence of the chemical composition over the AgNP stability and antimicrobial activity. In Figure 8, we display the AgNP antimicrobial activity ranges

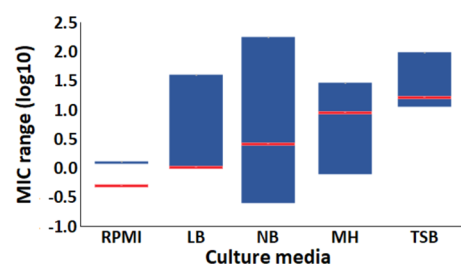


Figure 8. Culture media affect the antimicrobial activity of AgNPs. The AgNP minimal inhibitory concentration for *E. coli* is different in each culture medium, as can be observed in the ranges reported in the literature (blue bars) and our experimental results (red lines). Data are expressed as log₁₀.

on the logarithmic scale in the different culture media, organized by their chemical complexity. The blue bars represent the MIC ranges from the literature, whereas the red lines represent our punctual MIC values. The values from the literature and our experimental results are presented in Table S4.

This work reveals the importance of considering the culture medium conditions when assessing the AgNP antimicrobial activity. Also, it demonstrates that the AgNP antimicrobial potency from studies with the different experimental setups should not be directly compared as a comparison may be misleading. Finally, this approach could be potentially extended beyond AgNPs as there are many other nanoantibiotics under research.^{55,56}

As an additional observation, the literature review revealed that several studies regarding the antimicrobial activity provide a limited characterization of the AgNPs and/or limited information about the culture conditions. Most studies did not specify if the MIC values provided correspond to the estimated silver content or the total mass of the AgNPs when they are coated or otherwise modified. Most of the studies that were not considered for the meta-analysis lacked basic

information regarding the traits of the nanomaterials or about the susceptibility assays used.

3. CONCLUSIONS

Culture media play a critical role in the AgNP stability and antimicrobial activity. When AgNPs and *E. coli* from the same feedstock were tested under identical conditions, the MIC value changed up to 2 orders of magnitude by the effect of the culture media alone. Culture media influence AgNP physicochemical properties, such as hydrodynamic size, surface charge, silver ion release rate, and stability. Consequently, the antimicrobial potency of AgNPs is affected directly by the culture medium chemical complexity. The interactions and effects in the cell–nanoparticle–environment (culture conditions) system should be considered when assessing and interpreting the effect of AgNPs on the cell. Culture conditions are as relevant as the physicochemical traits of AgNPs when evaluating the antimicrobial potency of nanomaterials. Moreover, this study confirms that performing a comparative analysis to assess the antimicrobial potency or toxicity of AgNP data from the different reports could lead to misleading interpretations. More studies are still needed to expand the understanding of the role of the culture medium components on the AgNPs, particularly from the cell–nanomaterial–environment approach.

It is known that some strains require specific culture conditions; also, some experimental setups require particular arrangements in order to achieve their research aims. However, many research articles that only aim to assess the antimicrobial activities of nanomaterials, on common aerobic bacterial models, still use different culture conditions, such as culture media, inoculum size, initial incubation time, and temperature, among others. Moreover, in these studies, external controls are rarely used. For that reason, the authors emphasize that standardized protocols (CLSI, EUCAST, etc.) should be used whenever possible for assessing the antimicrobial activities of nanoparticles. Standardized protocols provide the advantage of facilitating reproducibility. Moreover, it facilitates comparing data across many different reports, allowing evaluation of the actual activity between nanomaterials, and even with common antibiotics. Additionally, experimental setups for nanomaterials that cannot follow standardized guidelines should include additional controls, such as the corresponding metallic ions, which may be a silver salt (AgNO₃) for AgNPs. Finally, our analysis of the current literature reveals that a vast majority of the published studies provide limited information regarding both the AgNP characterization and the conditions of antimicrobial susceptibility tests.

4. MATERIALS AND METHODS

4.1. Materials and Strains. **4.1.1. Silver Nanoparticles (AgNPs).** AgNPs were acquired from Vector Vita Ltd. (Novosibirsk, Russia). According to the manufacturer, these AgNPs are coated with polyvinylpyrrolidone (PVP) and are suspended in distilled water. These PVP–AgNPs were analyzed by transmission electron microscopy (TEM) (Figure S3). We found that the nanoparticles have an aspect ratio close to 1, with a metallic core diameter of 35 ± 15 nm.¹⁵ Moreover, a single-particle analysis revealed the crystalline arrangement of these nanoparticles.⁸ AgNPs were used as received, and the silver concentrations correspond to the silver content in the nanoparticles. For this study, we assessed the optical

characteristics of the AgNPs, as described in the corresponding sections (below).

4.1.2. Microorganism. The Gram-negative *E. coli* DH5 α bacterial strain was obtained from the microbial collection kept at the Centro de Nanociencias y Nanotecnología at the Universidad Nacional Autónoma de México. For the susceptibility assays, *E. coli* was subcultured in Mueller Hinton broth (MH) (BD Difco, MD) and incubated overnight, at 180 rpm, 37 °C.

4.1.3. Culture Media. The following culture media were prepared according to the standard formulations provided by the manufacturers: Roswell Park Memorial Institute (RPMI) 1640 medium from Sigma-Aldrich; Luria Bertani Broth (LB), Nutrient Broth (NB), Mueller Hinton Broth (MH), Yeast-Peptone-Dextrose Broth (YPD), and Tryptic-Soy Broth (TSB), all acquired from BD Difco (MD). The standard formulations for each culture medium are listed in the [Supporting Information](#) (List S1. Culture Media Broth Formulations).

4.2. Methods. **4.2.1. Effect of the Culture Medium Composition on the Stability of AgNPs.** To assess the impact of culture media on the AgNP stability, different sets of solutions were prepared in Milli-Q water, as follows: (a) peptone concentration gradient (0.58, 1.16, 1.75, 2.63, and 5.24%), pH 7.2; (b) dextrose concentration gradient (1 and 2%), pH 7.2; and (c) culture media: RPMI, LB, NB, MH, YPD, and TSB. Additionally, a set of Milli-Q water was adjusted to different pH values: 6.2, 7.2, and 8.2. All solutions were autoclaved, and then AgNPs were added in a final concentration of 50 $\mu\text{g mL}^{-1}$. As a control, AgNPs were also diluted in Milli-Q water, pH 7.2. All sets of solutions, with and without AgNPs, were incubated overnight, at 180 rpm, 37 °C, under sterile conditions. To ensure the reproducibility of results, solutions were prepared in triplicate.

4.2.2. Optical Characterization of the AgNPs. The effect of the different conditions in the AgNP size and stability was assessed at times 0 and 24 h.

4.2.2.1. UV–vis Spectrophotometry. 1 mL from each of the different AgNP solutions was transferred to a quartz cuvette and analyzed using a Multiskan Go spectrophotometer (Thermo Scientific), in a range of 275 to 700 nm, at room temperature. The corresponding solutions with no AgNPs were used as blanks. The collected data was used to graph the UV–vis profiles with the OriginPro 8 software (OriginLab).

4.2.2.2. Dynamic Light Scattering (DLS) Spectroscopy. The different AgNP solutions were transferred to a DTS 1060 folded capillary zeta cuvette. Then, the hydrodynamic diameter (HD) and the ζ -potential of the AgNPs were determined using a Zetasizer Nano NS (Malvern), at room temperature. The data was analyzed and graphed with OriginPro 8 (OriginLab).

4.2.3. Estimation of the Silver Release from the AgNPs over Time. The release of silver species over time from the AgNPs suspended in different culture media was assessed by inductively coupled plasma optical emission spectrometry (ICP-OES). Briefly, AgNPs were suspended in RPMI, MH, and YPD, for a final concentration of 10 $\mu\text{g mL}^{-1}$. For the time 0 h samples, the solutions were freshly prepared, whereas for the time 24 h samples, the solutions were incubated overnight, at 180 rpm, 37 °C, under sterile conditions. All samples were centrifuged for 15 min, at 5000 rpm. The supernatant was removed (then stored, see below), and the pellet was resuspended in 1 mL of Milli-Q water, and then it was sonicated and diluted with 9 mL of Milli-Q water. The silver

content from the resuspended pellet was measured using a Vista-MPX spectrometer (Varian). Regarding the supernatants from the different samples, they were kept in a sealed, light-protected container, at 4 °C, until they were analyzed. The supernatants were examined to determine the potential presence of AgNPs and non-nanostructured silver. Briefly, 1 mL of the supernatants was transferred to quartz cuvettes and analyzed via UV–vis spectrophotometry, in a range of 275 to 700 nm, at room temperature, using a Multiskan Go spectrophotometer (Thermo Scientific). The corresponding culture media, also centrifuged and with no AgNPs, were used as blanks. To confirm the reproducibility of the results, ICP-OES was performed in duplicate for each condition. Data were analyzed with the OriginPro 8 software (OriginLab). The silver content from the pellets was analyzed via one-way ANOVA followed by Tukey's multiple comparison post-test, whereas the data collected from supernatants were graphed to build the UV–vis profiles.

4.2.4. coli Growth under Different Culture Conditions. The growth of *E. coli* under the different culture media was evaluated. Briefly, *E. coli* from the overnight MH cultures was adjusted to 10⁶ cells mL⁻¹ and then subcultured under the following conditions, in triplicate: (a) modified MH broth: different peptone concentrations: 0.58, 1.16, 1.75 (standard), 2.63, and 5.24% and different dextrose concentrations: 0 (standard), 1, and 2%; (b) liquid culture media: RPMI 1640, NB, LB, MH, and YPD. Subsequently, *E. coli* was incubated in standard conditions (37 °C, 24 h, 180 rpm). The microbial growth was determined by measuring the optical absorbance at $\lambda = 600$ nm, using the corresponding untreated culture media as the blank, with a Multiskan Go spectrophotometer (Thermo Scientific). The absorbance values were converted to the percentage of growth. *E. coli* growth from the unmodified MH formulation was set as the reference (100%). The statistical analysis was performed via one-way ANOVA with Tukey's multiple comparison post-test, with the OriginPro 8 software (OriginLab).

4.2.5. Effect of Culture Conditions on the Antimicrobial Activity of the AgNPs. The antibacterial activity of AgNPs was assessed following the guidelines of the CLSI M09-A7 protocols,⁵⁷ with variations in the culture media. From the overnight cultures, *E. coli* was washed with PBS and adjusted to 10⁶ cells mL⁻¹ in the different culture media, as follows: (a) modified MH broth: different peptone concentrations: 0.58, 1.16, 1.75, 2.63, and 5.24% and different dextrose concentrations: 0, 1, and 2%; (b) liquid culture media: RPMI 1640, NB, LB, MH, YPD, and TSB. Then AgNPs were added into the 96 multiwell plates, in a concentration range of 7.5 to 20 $\mu\text{g mL}^{-1}$ (in 2.5 $\mu\text{g mL}^{-1}$ serial steps) and incubated in standard conditions (37 °C, 24 h, 180 rpm). The minimal inhibitory concentration (MIC) was set as the concentration where no visible growth was observed. The reported AgNP MIC values are the ones that were more commonly observed. However, in some cases, the AgNP MIC values were within one step of the reported value. To ensure reproducibility, three biological susceptibility assays were performed in 96-multiwell plates, with duplicates of each condition within each plate.

4.2.6. Meta-Analysis of the AgNP MIC Ranges in Different Culture Media. To assess any potential correlation between the AgNP MIC values and the culture media, a meta-analysis from the published MIC values was performed. Original research articles were chosen according to the following criteria: use of an *E. coli* strain, mention the quantitative size of

the initial inoculum, mention/describe the culture media, use of a microdilution method for the susceptibility assays (and describe it), and explicitly display the MIC value (mass/volume, moles, ppm, or any other equivalent). More than 400 original research articles were evaluated (antibacterial AgNPs vs *E. coli*); from these, less than 10% met all the criteria.^{10,11,15,19,21,22,33,35,39,42,53,58–84} MICs were organized by culture media, and their MIC range within each group was calculated. Finally, our experimental AgNP MIC values were contrasted with the meta-analysis to compare them with the trending data.

■ ASSOCIATED CONTENT

SI Supporting Information

The Supporting Information is available free of charge at <https://pubs.acs.org/doi/10.1021/acsomega.0c02007>.

UV–vis spectra, TEM micrographs, hydrodynamic size and DLS characterization of AgNPs. Culture medium broth major composition. Silver content determination by ICP-OES. AgNP MIC on *E. coli* in different culture media (PDF)

■ AUTHOR INFORMATION

Corresponding Author

Alejandro Huerta-Saquero – Centro de Nanociencias y Nanotecnología, Universidad Nacional Autónoma de México, CP 22860 Ensenada, Baja California, México; orcid.org/0000-0002-0156-6773; Email: saquero@cnyunam.mx

Authors

Roberto Vazquez-Muñoz – Department of Biology and The South Texas Center for Emerging Infectious Diseases, The University of Texas at San Antonio, San Antonio, Texas 78249, United States; Centro de Nanociencias y Nanotecnología, Universidad Nacional Autónoma de México, CP 22860 Ensenada, Baja California, México; orcid.org/0000-0002-3847-1305

Nina Bogdanchikova – Centro de Nanociencias y Nanotecnología, Universidad Nacional Autónoma de México, CP 22860 Ensenada, Baja California, México

Complete contact information is available at: <https://pubs.acs.org/doi/10.1021/acsomega.0c02007>

Notes

The authors declare no competing financial interest.

■ ACKNOWLEDGMENTS

We would like to thank the CONACyT for R.V.-M.'s doctoral fellowship. This work was supported by DGAPA Grant IN210618 and CONACyT grants 284385 and SINANOTOX PN-2017-01-4710 (A.H.-S.). N.B. thanks the International Bionanotechnology Network. We also thank Dr. Katrin Quester and Itandehui Betanzo for technical assistance.

■ REFERENCES

- (1) Zivic, F.; Grujovic, N.; Mitrovic, S.; Ahad, I. U.; Brabazon, D. Characteristics and Applications of Silver Nanoparticles. In *Commercialization of Nanotechnologies—A Case Study Approach*; Brabazon, D., Pellicer, E., Zivic, F., Sort, J., Dolores Baró, M., Grujovic, N., Choy, K.-L., Eds.; Springer International Publishing: Cham, 2018; pp. 227–273, DOI: 10.1007/978-3-319-56979-6_10.
- (2) Vance, M. E.; Kuiken, T.; Vejerano, E. P.; McGinnis, S. P.; Hochella, M. F., Jr.; Rejeski, D.; Hull, M. S. Nanotechnology in the

Real World: Redeveloping the Nanomaterial Consumer Products Inventory. *Beilstein J. Nanotechnol.* **2015**, *6*, 1769–1780.

(3) Syafuddin, A.; Salmiati; Salim, M. R.; Beng Hong Kueh, A.; Hadibarata, T.; Nur, H. A Review of Silver Nanoparticles: Research Trends, Global Consumption, Synthesis, Properties, and Future Challenges. *J. Chin. Chem. Soc.* **2017**, *64*, 732–756.

(4) Lara, H. H.; Garza-Treviño, E. N.; Ixtapan-Turrent, L.; Singh, D. K. Silver Nanoparticles Are Broad-Spectrum Bactericidal and Virucidal Compounds. *J. Nanobiotechnol.* **2011**, *9*, 30.

(5) Bogdanchikova, N.; Muñoz, R. V.; Saquero, A. H.; Jasso, A. P.; Uzcanga, G. A.; Díaz, P. L. P.; Pestryakov, A.; Burmistrov, V.; Martynyuk, O.; Gómez, R. L. V.; Almanza, H. Silver Nanoparticles Composition for Treatment of Distemper in Dogs. *Int. J. Nanotechnol.* **2016**, *13*, 227.

(6) Jaime-Acuña, O. E.; Meza-Villecas, A.; Vasquez-Peña, M.; Raymond-Herrera, O.; Villavicencio-García, H.; Petranovskii, V.; Vazquez-Duhalt, R.; Huerta-Saquero, A. Synthesis and Complete Antimicrobial Characterization of CEOBACTER, an Ag-Based Nanocomposite. *PLoS One* **2016**, *11*, e0166205–e0166218.

(7) Vazquez-Muñoz, R.; Arellano-Jimenez, M. J.; Lopez, F. D.; Lopez-Ribot, J. L. Protocol Optimization for a Fast, Simple and Economical Chemical Reduction Synthesis of Antimicrobial Silver Nanoparticles in Non-Specialized Facilities. *BMC Res. Notes* **2019**, *12*, 773.

(8) Vazquez-Muñoz, R.; Avalos-Borja, M.; Castro-Longoria, E. Ultrastructural Analysis of *Candida Albicans* When Exposed to Silver Nanoparticles. *PLoS One* **2014**, *9*, No. e108876.

(9) Lara, H. H.; Ixtapan-Turrent, L.; Jose Yacamán, M.; Lopez-Ribot, J. Inhibition of *Candida Auris* Biofilm Formation on Medical and Environmental Surfaces by Silver Nanoparticles. *ACS Appl. Mater. Interfaces* **2020**, *12*, 21183.

(10) Fayaz, A. M.; Balaji, K.; Girilal, M.; Yadav, R.; Kalachelvan, P. T.; Venketesan, R. Biogenic Synthesis of Silver Nanoparticles and Their Synergistic Effect with Antibiotics: A Study against Gram-Positive and Gram-Negative Bacteria. *Nanomed. Nanotechnol., Biol. Med.* **2010**, *6*, 103–109.

(11) Vazquez-Muñoz, R.; Meza-Villecas, A.; Fournier, P. G. J.; Soria-Castro, E.; Juárez-Moreno, K.; Gallego-Hernández, A. L.; Bogdanchikova, N.; Vazquez-Duhalt, R.; Huerta-Saquero, A. Enhancement of Antibiotics Antimicrobial Activity Due to the Silver Nanoparticles Impact on the Cell Membrane. *PLoS One* **2019**, *14*, No. e0224904.

(12) Li, P.; Li, J.; Wu, C.; Wu, Q.; Li, J. Synergistic Antibacterial Effects of β -Lactam Antibiotic Combined with Silver Nanoparticles. *Nanotechnology* **2005**, *16*, 1912–1917.

(13) European Chemicals Agency. *Guidance on Information Requirements and Chemical Safety Assessment. Chapter R7a: Endpoint Specific Guidance*; 2016, DOI: 10.2823/2611.

(14) Kubo, A. L.; Capjak, I.; Vrček, I. V.; Bondarenko, O. M.; Kurvet, I.; Vija, H.; Ivask, A.; Kasemets, K.; Kahru, A. Antimicrobial Potency of Differently Coated 10 and 50 nm Silver Nanoparticles against Clinically Relevant Bacteria *Escherichia Coli* and *Staphylococcus Aureus*. *Colloids Surf., B* **2018**, *170*, 401–410.

(15) Vazquez-Muñoz, R.; Borrego, B.; Juárez-Moreno, K.; García-García, M.; Mota Morales, J. D.; Bogdanchikova, N.; Huerta-Saquero, A. Toxicity of Silver Nanoparticles in Biological Systems: Does the Complexity of Biological Systems Matter? *Toxicol. Lett.* **2017**, *276*, 11–20.

(16) You, J.; Zhang, Y.; Hu, Z. Bacteria and Bacteriophage Inactivation by Silver and Zinc Oxide Nanoparticles. *Colloids Surf., B* **2011**, *85*, 161–167.

(17) Anwar, A.; Masri, A.; Rao, K.; Rajendran, K.; Khan, N. A.; Shah, M. R.; Siddiqui, R. Antimicrobial Activities of Green Synthesized Gums-Stabilized Nanoparticles Loaded with Flavonoids. *Sci. Rep.* **2019**, *9*, 1–12.

(18) Vargas-Reus, M. A.; Memarzadeh, K.; Huang, J.; Ren, G. G.; Allaker, R. P. Antimicrobial Activity of Nanoparticulate Metal Oxides against Peri-Implantitis Pathogens. *Int. J. Antimicrob. Agents* **2012**, *40*, 135–139.

- (19) Pallavicini, P.; Arciola, C. R.; Bertoglio, F.; Curtosi, S.; Dacarro, G.; D'Agostino, A.; Ferrari, F.; Merli, D.; Milanese, C.; Rossi, S.; Taglietti, A.; Tenci, M.; Visai, L. Silver Nanoparticles Synthesized and Coated with Pectin: An Ideal Compromise for Anti-Bacterial and Anti-Biofilm Action Combined with Wound-Healing Properties. *J. Colloid Interface Sci.* **2017**, *498*, 271–281.
- (20) Acharya, D.; Malabika Singha, K.; Pandey, P.; Mohanta, B.; Rajkumari, J. Paikhomba Singha, & L. Shape Dependent Physical Mutilation and Lethal Effects of Silver Nanoparticles on Bacteria OPEN. *Sci. Rep.* **2018**, *8*, 201.
- (21) Tahir, K.; Ahmad, A.; Li, B.; Nazir, S.; Khan, A. U.; Nasir, T.; Khan, Z. U. H.; Naz, R.; Raza, M. Visible Light Photo Catalytic Inactivation of Bacteria and Photo Degradation of Methylene Blue with Ag/TiO₂ Nanocomposite Prepared by a Novel Method. *J. Photochem. Photobiol. B Biol.* **2016**, *162*, 189–198.
- (22) Ruparelia, J. P.; Chatterjee, A. K.; Duttagupta, S. P.; Mukherji, S. Strain Specificity in Antimicrobial Activity of Silver and Copper Nanoparticles. *Acta Biomater.* **2008**, *4*, 707–716.
- (23) McShan, D.; Ray, P. C.; Yu, H. Molecular Toxicity Mechanism of Nanosilver. *J. Food Drug Anal.* **2014**, *22*, 116–127.
- (24) Tejamaya, M.; Römer, I.; Merrifield, R. C.; Lead, J. R. Stability of Citrate, PVP, and PEG Coated Silver Nanoparticles in Ecotoxicology Media. *Environ. Sci. Technol.* **2012**, *46*, 7011–7017.
- (25) Delay, M.; Dolt, T.; Woellhaf, A.; Sembritzki, R.; Frimmel, F. H. Interactions and Stability of Silver Nanoparticles in the Aqueous Phase: Influence of Natural Organic Matter (NOM) and Ionic Strength. *J. Chromatogr. A* **2011**, *1218*, 4206–4212.
- (26) Juling, S.; Niedzwiecka, A.; Böhmert, L.; Lichtenstein, D.; Selve, S.; Braeuning, A.; Thünemann, A. F.; Krause, E.; Lampen, A. Protein Corona Analysis of Silver Nanoparticles Links to Their Cellular Effects. *J. Proteome Res.* **2017**, *16*, 4020–4034.
- (27) Lundqvist, M.; Stigler, J.; Elia, G.; Lynch, I.; Cedervall, T.; Dawson, K. A. Nanoparticle Size and Surface Properties Determine the Protein Corona with Possible Implications for Biological Impacts. *Proc. Natl. Acad. Sci.* **2008**, *105*, 14265–14270.
- (28) Gnanadhas, D. P.; Ben Thomas, M.; Thomas, R.; Raichur, A. M.; Chakravorty, D. Interaction of Silver Nanoparticles with Serum Proteins Affects Their Antimicrobial Activity in Vivo. *Antimicrob. Agents Chemother.* **2013**, *57*, 4945–4955.
- (29) Chung, Y. C.; Chen, I. H.; Chen, C. J. The Surface Modification of Silver Nanoparticles by Phosphoryl Disulfides for Improved Biocompatibility and Intracellular Uptake. *Biomaterials* **2008**, *29*, 1807–1816.
- (30) Seitz, F.; Rosenfeldt, R. R.; Storm, K.; Metreveli, G.; Schaumann, G. E.; Schulz, R.; Bundschuh, M. Effects of Silver Nanoparticle Properties, Media PH and Dissolved Organic Matter on Toxicity to *Daphnia Magna*. *Ecotoxicol. Environ. Saf.* **2015**, *111*, 263–270.
- (31) De Leersnyder, I.; De Gelder, L.; Van Driessche, I.; Vermeir, P. Influence of Growth Media Components on the Antibacterial Effect of Silver Ions on *Bacillus Subtilis* in a Liquid Growth Medium. *Sci. Rep.* **2018**, *8*, 9325.
- (32) Wigginton, N. S.; de Titta, A.; Piccapietra, F.; Dobias, J.; Nesatyy, V. J.; Suter, M. J. F.; Bernier-Latmani, R. Binding of Silver Nanoparticles to Bacterial Proteins Depends on Surface Modifications and Inhibits Enzymatic Activity. *Environ. Sci. Technol.* **2010**, *44*, 2163–2168.
- (33) Greulich, C.; Braun, D.; Peetsch, A.; Diendorf, J.; Siebers, B.; Epple, M.; Köller, M. The Toxic Effect of Silver Ions and Silver Nanoparticles towards Bacteria and Human Cells Occurs in the Same Concentration Range. *RSC Adv.* **2012**, *2*, 6981.
- (34) Fabrega, J.; Luoma, S. N.; Tyler, C. R.; Galloway, T. S.; Lead, J. R. Silver Nanoparticles: Behaviour and Effects in the Aquatic Environment. *Environ. Int.* **2011**, *37*, 517–531.
- (35) Goswami, S. R.; Sahareen, T.; Singh, M.; Kumar, S. Role of Biogenic Silver Nanoparticles in Disruption of Cell–Cell Adhesion in *Staphylococcus Aureus* and *Escherichia Coli* Biofilm. *J. Ind. Eng. Chem.* **2015**, *26*, 73–80.
- (36) Fabrega, J.; Fawcett, S. R.; Renshaw, J. C.; Lead, J. R. Silver Nanoparticle Impact on Bacterial Growth: Effect of PH, Concentration, and Organic Matter. *Environ. Sci. Technol.* **2009**, *43*, 7285–7290.
- (37) Qu, F.; Xu, H.; Wei, H.; Lai, W.; Xiong, Y.; Xu, F.; Aguilar, Z. P.; Xu, H.; Wang, Y. A. Effects of PH and Temperature on Antibacterial Activity of Silver Nanoparticles. *2010 3rd Int. Conf. Biomed. Eng. Informatics*; 2010, No. Bmei, 2033–2037, DOI: 10.1109/BMEI.2010.5639483.
- (38) MacCuspie, R. I. Colloidal Stability of Silver Nanoparticles in Biologically Relevant Conditions. *J. Nanopart. Res.* **2011**, *13*, 2893–2908.
- (39) Jadalannagari, S.; Deshmukh, K.; Ramanan, S. R.; Kowshik, M. Antimicrobial Activity of Hemocompatible Silver Doped Hydroxyapatite Nanoparticles Synthesized by Modified Sol–Gel Technique. *Appl. Nanosci.* **2014**, *4*, 133–141.
- (40) Mahendiran, D.; Kumar, R. S.; Rahiman, A. K. Heteroleptic Silver(I) Complexes with 2,2':6',2''-Terpyridines and Naproxen: DNA Interaction, EGFR/VEGFR2 Kinase, Growth Inhibition and Cell Cycle Arrest Studies. *Mater. Sci. Eng. C* **2017**, *76*, 601–615.
- (41) Baset, S.; Akbari, H.; Zeynali, H.; Shafie, M. Size Measurement of Metal and Semiconductor Nanoparticles via UV-Vis Absorption Spectra. *Dig. J. Nanomater. Biostructures* **2011**, *6*, 709–716.
- (42) Agnihotri, S.; Mukherji, S.; Mukherji, S. Size-Controlled Silver Nanoparticles Synthesized over the Range 5–100 Nm Using the Same Protocol and Their Antibacterial Efficacy. *RSC Adv.* **2014**, *4*, 3974–3983.
- (43) Liao, S. Y.; Read, D. C.; Pugh, W. J.; Furr, J. R.; Russell, A. D. Interaction of Silver Nitrate with Readily Identifiable Groups: Relationship to the Antibacterial Action of Silver Ions. *Lett. Appl. Microbiol.* **1997**, *25*, 279–283.
- (44) Loza, K.; Diendorf, J.; Sengstock, C.; Ruiz-Gonzalez, L.; Gonzalez-Calbet, J. M.; Vallet-Regi, M.; Köller, M.; Epple, M. The Dissolution and Biological Effects of Silver Nanoparticles in Biological Media. *J. Mater. Chem. B* **2014**, *2*, 1634.
- (45) Navarro, E.; Piccapietra, F.; Wagner, B.; Marconi, F.; Kaegi, R.; Odzak, N.; Sigg, L.; Behra, R. Toxicity of Silver Nanoparticles to *Chlamydomonas Reinhardtii*. *Environ. Sci. Technol.* **2008**, *42*, 8959–8964.
- (46) Boehmler, D. J.; O'Dell, Z. J.; Chung, C.; Riley, K. R. Bovine Serum Albumin Enhances Silver Nanoparticle Dissolution Kinetics in a Size- And Concentration-Dependent Manner. *Langmuir* **2020**, *36*, 1053–1061.
- (47) Yallapu, M. M.; Chauhan, N.; Othman, S. F.; Khalilzad-Sharghi, V.; Ebeling, M. C.; Khan, S.; Jaggi, M.; Chauhan, S. C. Implications of Protein Corona on Physico-Chemical and Biological Properties of Magnetic Nanoparticles. *Biomaterials* **2015**, *46*, 1–12.
- (48) de Barros, C. H. N.; Cruz, G.; Mayrink, W.; Tasic, L. Bio-Based Synthesis of Silver Nanoparticles from Orange Waste: Effects of Distinct Biomolecule Coatings on Size, Morphology, and Antimicrobial Activity. *Nanotechnol. Sci. Appl.* **2018**, *Volume 11*, 1–14.
- (49) Prathna, T. C.; Chandrasekaran, N.; Mukherjee, A. Studies on Aggregation Behaviour of Silver Nanoparticles in Aqueous Matrices: Effect of Surface Functionalization and Matrix Composition. *Colloids Surf., A* **2011**, *390*, 216–224.
- (50) Haider, M. J.; Mehdi, M. S. Study of Morphology and Zeta Potential Analyzer for the Silver Nanoparticles. *Int. J. Sci. Eng. Res.* **2014**, *5*, 381.
- (51) Koczur, K. M.; Mourdikoudis, S.; Polavarapu, L.; Skrabalak, S. E. Polyvinylpyrrolidone (PVP) in Nanoparticle Synthesis. *Dalton Trans.* **2015**, *44*, 17883.
- (52) Danaei, M.; Dehghankhold, M.; Ataei, S.; Hasanzadeh Davarani, F.; Javanmard, R.; Dokhani, A.; Khorasani, S.; Mozafari, M. R. Impact of Particle Size and Polydispersity Index on the Clinical Applications of Lipidic Nanocarrier Systems. In *Pharmaceutics* MDPI AG May 10, 2018, p 57, DOI: 10.3390/pharmaceutics10020057.
- (53) Kvítek, L.; Panáček, A.; Soukupová, J.; Kolář, M.; Večeřová, R.; Prucek, R.; Holecová, M.; Zbořil, R. *Effect of Surfactants and Polymers*

on Stability and Antibacterial Activity of Silver Nanoparticles (NPs); 2008, DOI: 10.1021/jp711616v.

(54) Mohan, S.; Oluwafemi, O. S.; George, S. C.; Jayachandran, V. P.; Lewu, F. B.; Songca, S. P.; Kalarikkal, N.; Thomas, S. Completely Green Synthesis of Dextrose Reduced Silver Nanoparticles, Its Antimicrobial and Sensing Properties. *Carbohydr. Polym.* **2014**, *106*, 469–474.

(55) Vazquez-Munoz, R.; Arellano-Jimenez, M. J.; Lopez-Ribot, J. Bismuth Nanoparticles Obtained by a Facile Synthesis Method Exhibit Antimicrobial Activity against Staphylococcus Aureus and Candida Albicans. *bioRxiv*; 2020, DOI: 10.1101/2020.06.05.137109.

(56) Muzammil, S.; Hayat, S.; Fakhar-E-Alam, M.; Aslam, B.; Siddique, M. H.; Nisar, M. A.; Saqalein, M.; Atif, M.; Sarwar, A.; Khurshid, A.; Amin, N.; Wang, Z. Nanoantibiotics: Future Nanotechnologies to Combat Antibiotic Resistance. *Front. Biosci., Elite Ed.* **2018**, *10*, 352–374.

(57) CLSI. *M07. Methods for Dilution Antimicrobial Susceptibility Tests for Bacteria That Grow Aerobically*; 11th ed.; Weinstein, M. P., Ed.; Wayne, PA: 2018.

(58) Lok, C.-N.; Ho, C.-M.; Chen, R.; He, Q.-Y.; Yu, W.-Y.; Sun, H.; Tam, P. K.-H.; Chiu, J.-F.; Che, C.-M. Silver Nanoparticles: Partial Oxidation and Antibacterial Activities. *JBIC, J. Biol. Inorg. Chem.* **2007**, *12*, 527–534.

(59) Peetsch, A.; Greulich, C.; Braun, D.; Stroetges, C.; Rehage, H.; Siebers, B.; Köller, M.; Epple, M. Silver-Doped Calcium Phosphate Nanoparticles: Synthesis, Characterization, and Toxic Effects toward Mammalian and Prokaryotic Cells. *Colloids Surf., B* **2013**, *102*, 724–729.

(60) Radzig, M. A.; Nadtochenko, V. A.; Koksharova, O. A.; Kiwi, J.; Lipasova, V. A.; Khmel, I. A. Antibacterial Effects of Silver Nanoparticles on Gram-Negative Bacteria: Influence on the Growth and Biofilms Formation, Mechanisms of Action. *Colloids Surf., B* **2013**, *102*, 300–306.

(61) Liu, H.-L.; Dai, S. A.; Fu, K.-Y.; Hsu, S.-H. Antibacterial Properties of Silver Nanoparticles in Three Different Sizes and Their Nanocomposites with a New Waterborne Polyurethane. *Int. J. Nanomed.* **2010**, *5*, 1017–1028.

(62) Xia, Q.; Ma, Y.; Wang, J.; Xia, Q. H.; Ma, Y. J.; Wang, J. W. Biosynthesis of Silver Nanoparticles Using Taxus Yunnanensis Callus and Their Antibacterial Activity and Cytotoxicity in Human Cancer Cells. *Nanomaterials* **2016**, *6*, 160.

(63) Ninganagouda, S.; Rathod, V.; Singh, D.; Hiremath, J.; Singh, A. K.; Mathew, J.; ul-Haq, M. Growth Kinetics and Mechanistic Action of Reactive Oxygen Species Released by Silver Nanoparticles from Aspergillus Niger on Escherichia Coli. *Biomed Res. Int.* **2014**, *2014*, 753419.

(64) Pal, S.; Tak, Y. K.; Song, J. M. Does the Antibacterial Activity of Silver Nanoparticles Depend on the Shape of the Nanoparticle? A Study of the Gram-Negative Bacterium Escherichia Coli. *Appl. Environ. Microbiol.* **2007**, *73*, 1712–1720.

(65) Raffi, M.; Hussain, F.; Bhatti, T. M.; Akhter, J. I.; Hameed, A.; Hasan, M. M. *Antibacterial Characterization of Silver Nanoparticles against E. coli ATCC-15224*; 2008; Vol. 24.

(66) Zhang, Y.; Peng, H.; Huang, W.; Zhou, Y.; Yan, D. Facile Preparation and Characterization of Highly Antimicrobial Colloid Ag or Au Nanoparticles. *J. Colloid Interface Sci.* **2008**, *325*, 371–376.

(67) Ivask, A.; Elbadawy, A.; Kaweeteerawat, C.; Boren, D.; Fischer, H.; Ji, Z.; Chang, C. H.; Liu, R.; Tolaymat, T.; Telesca, D.; Zink, J. L.; Cohen, Y.; Holden, P. A.; Godwin, H. A. Toxicity Mechanisms in Escherichia Coli Vary for Silver Nanoparticles and Differ from Ionic Silver. *ACS Nano* **2014**, *8*, 374–386.

(68) Li, D.; Liu, Z.; Yuan, Y.; Liu, Y.; Niu, F. Green Synthesis of Gallic Acid-Coated Silver Nanoparticles with High Antimicrobial Activity and Low Cytotoxicity to Normal Cells. *Process Biochem.* **2015**, *50*, 357–366.

(69) Zhang, S.; Liu, L.; Pareek, V.; Becker, T.; Liang, J.; Liu, S. Effects of Broth Composition and Light Condition on Antimicrobial Susceptibility Testing of Ionic Silver. *J. Microbiol. Methods* **2014**, *105*, 42–46.

(70) Ansari, M. A.; Khan, H. M.; Khan, A. A.; Ahmad, M. K.; Mahdi, A. A.; Pal, R.; Cameotra, S. S. Interaction of Silver Nanoparticles with Escherichia Coli and Their Cell Envelope Biomolecules. *J. Basic Microbiol.* **2014**, *54*, 905–915.

(71) Shrivastava, S.; Bera, T.; Roy, A.; Singh, G.; Ramachandrarao, P.; Dash, D. Characterization of Enhanced Antibacterial Effects of Novel Silver Nanoparticles. *Nanotechnology* **2007**, *18*, 225103.

(72) Li, P.; Li, J.; Wu, C.; Wu, Q.; Li, J. Synergistic Antibacterial Effects of β -Lactam Antibiotic Combined with Silver Nanoparticles. *Nanotechnology* **2005**, *16*, 1912–1917.

(73) Orłowski, P.; Zmigrodzka, M.; Tomaszewska, E.; Ransozek-Soliwoda, K.; Czupryn, M.; Antos-Bielska, M.; Szemraj, J.; Celichowski, G.; Grobelny, J.; Krzyzowska, M. Tannic Acid-Modified Silver Nanoparticles for Wound Healing: The Importance of Size. *Int. J. Nanomed.* **2018**, *13*, 991–1007.

(74) Annadhasan, M.; SankarBabu, V. R.; Naresh, R.; Umamaheswari, K.; Rajendiran, N. A Sunlight-Induced Rapid Synthesis of Silver Nanoparticles Using Sodium Salt of N-Cholyl Amino Acids and Its Antimicrobial Applications. *Colloids Surf., B* **2012**, *96*, 14–21.

(75) Panáček, A.; Kvítek, L.; Smékalová, M.; Večeřová, R.; Kolář, M.; Röderová, M.; Dyčka, F.; Šebela, M.; Pucek, R.; Tomanec, O.; Zbořil, R. Bacterial Resistance to Silver Nanoparticles and How to Overcome It. *Nat. Nanotechnol.* **2018**, *13*, 65–71.

(76) Suchomel, P.; Kvítek, L.; Panacek, A.; Pucek, R.; Hrbac, J.; Vecerova, R.; Zboril, R. Comparative Study of Antimicrobial Activity of AgBr and Ag Nanoparticles (NPs). *PLoS One* **2015**, *10*, e0119202–e0119216.

(77) Martínez-Castañón, G. A.; Niño-Martínez, N.; Martínez-Gutiérrez, F.; Martínez-Mendoza, J. R.; Ruiz, F. Synthesis and Antibacterial Activity of Silver Nanoparticles with Different Sizes. *J. Nanopart. Res.* **2008**, *10*, 1343–1348.

(78) Pucek, R.; Tuček, J.; Kiliánová, M.; Panáček, A.; Kvítek, L.; Filip, J.; Kolář, M.; Tománková, K.; Zbořil, R. The Targeted Antibacterial and Antifungal Properties of Magnetic Nanocomposite of Iron Oxide and Silver Nanoparticles. *Biomaterials* **2011**, *32*, 4704–4713.

(79) Li, W.-R.; Xie, X.-B.; Shi, Q.-S.; Zeng, H.-Y.; Ou-Yang, Y.-S.; Chen, Y.-B. Antibacterial Activity and Mechanism of Silver Nanoparticles on Escherichia Coli. *Appl. Microbiol. Biotechnol.* **2010**, *85*, 1115–1122.

(80) Nogueira, S. S.; de Araujo-Nobre, A. R.; Mafud, A. C.; Guimarães, M. A.; Alves, M. M. M.; Plácido, A.; Carvalho, F. A. A.; Arcanjo, D. D. R.; Mascarenhas, Y.; Costa, F. G.; Albuquerque, P.; Eaton, P.; de Souza de Almeida Leite, J. R.; da Silva, D. A.; Cardoso, V. S. Silver Nanoparticle Stabilized by Hydrolyzed Collagen and Natural Polymers: Synthesis, Characterization and Antibacterial-Antifungal Evaluation. *Int. J. Biol. Macromol.* **2019**, *135*, 808–814.

(81) Kanmani, P.; Lim, S. T. Synthesis and Characterization of Pullulan-Mediated Silver Nanoparticles and Its Antimicrobial Activities. *Carbohydr. Polym.* **2013**, *97*, 421–428.

(82) Paredes, D.; Ortiz, C.; Torres, R. Synthesis, Characterization, and Evaluation of Antibacterial Effect of Ag Nanoparticles against Escherichia Coli O157:H7 and Methicillin-Resistant Staphylococcus Aureus (MRSA). *Int. J. Nanomed.* **2014**, *9*, 1717–1729.

(83) Martínez-Gutiérrez, F.; Olive, P. L.; Banuelos, A.; Orrantia, E.; Nino, N.; Sanchez, E. M.; Ruiz, F.; Bach, H.; Av-Gay, Y. Synthesis, Characterization, and Evaluation of Antimicrobial and Cytotoxic Effect of Silver and Titanium Nanoparticles. *Nanomed.: Nanotechnol., Biol. Med.* **2010**, *6*, 681–688.

(84) Martínez-Gutiérrez, F.; Thi, E. P.; Silverman, J. M.; de Oliveira, C. C.; Svensson, S. L.; Hoek, A.; Vanden; Sánchez, E. M.; Reiner, N. E.; Gaynor, E. C.; Pryzdial, E. L. G.; Conway, E. M.; Orrantia, E.; Ruiz, F.; Av-Gay, Y.; Bach, H. Antibacterial Activity, Inflammatory Response, Coagulation and Cytotoxicity Effects of Silver Nanoparticles. *Nanomed.: Nanotechnol., Biol. Med.* **2012**, *8*, 328–336.